Acta Biomaterialia 7 (2011) 3955–3963

Contents lists available at ScienceDirect

Acta Biomaterialia

journal homepage: www.elsevier.com/locate/actabiomat

Multifunctional alginate microspheres for biosensing, drug delivery and magnetic resonance imaging

Abhijeet Joshi [a,1], Sanket Solanki [a,1], Rashmi Chaudhari [a,1], Dhirendra Bahadur [b], M. Aslam [c], Rohit Srivastava [a,*]

[a] Department of Biosciences and Bioengineering, IIT Bombay, Powai, Mumbai, 400 076 Maharashtra, India
[b] Department of Metallurgical Engineering and Material Science, IIT Bombay, Powai, Mumbai, 400 076 Maharashtra, India
[c] Department of Physics, IIT Bombay, Powai, Mumbai, 400 076 Maharashtra, India

ARTICLE INFO

Article history:
Received 3 March 2011
Received in revised form 17 June 2011
Accepted 30 June 2011
Available online 8 July 2011

Keywords:
Magnetic nanoparticles
Alginate microspheres
Biosensor
Drug delivery
MRI

ABSTRACT

This research aims to develop and investigate a multifunctional implantable system capable of biosensing, drug delivery and magnetic resonance imaging (MRI) for continuous monitoring, controlled anti-inflammatory drug delivery and imaging, respectively. A glucose biosensor, diclofenac sodium (Diclo) and magnetic nanoparticles (MNP) were used as the biosensor component, anti-inflammatory agent and MRI contrast agent, respectively. MNP were synthesized by the co-precipitation technique and loaded with the sensor and drug components into alginate microspheres using a commercial droplet generator. The multifunctional system was then characterized using optical microscopy, scanning electron microscopy, transmission electron microscopy, X-ray diffraction, vibrating sample magnetometry (VSM) and MRI. The MNP were found to be in the size range of 5–15 nm. The final system, comprising the biosensor, drug and MNP loaded inside alginate microspheres, was found to be in the size range of 10–60 μm. Biosensing studies indicated an excellent glucose response curve, with a regression coefficient of 0.974 (0–10 mM of glucose, response time: 4 min). In vitro Diclo release shows that MNP loading in alginate microspheres increases the burst release percentage by 11–12% in both 60 and 10 μm particles. However, the duration of release for 85% drug release decreases with MNP loading by 7 and 6 days for 39 the 60 and 10 μm particles, respectively. Super-paramagnetism was confirmed by VSM, with 2.09 and 1.368 emu g^{-1}, respectively, for the 60 and 10 μm particles, with no hysteresis. MRI showed significant contrast for both sizes. The particles showed an excellent biocompatibility (>80%) for all combinations of formulations. The system shows a great potential for biosensing with concurrent drug delivery and visualization for biomedical applications.

1. Introduction

Implantable devices, such as biosensors, drug delivery devices, catheters and microdialysis probes have a wide range of applications in clinical diagnosis and treatment. Implantable biosensors form important devices which can be used for continuous monitoring of various analytes present in the blood. Many additional components like therapeutic agents and magnetic resonance imaging (MRI) agents can be co-immobilized/co-administered with the implanted biosensor to maintain and improve functionality [1]. In the recent past, several implantable glucose biosensors have been developed but closed-loop glucose detection and treatment seem a remote possibility. Due to insufficient accuracy and reliability of non-invasive and minimally invasive glucose biosensors, designing a biosensor for subcutaneous implantation, like "Smart Tattoo", appears to be the best choice for effective disease management [2]. Major problems associated with implantable biosensors are that they progressively lose functionality when they are implanted *in vivo*, which is mainly attributed to host tissue response due to changes in the tissue environment. Implantation results in an immune response which takes the form of a cascade of reactions of protein and inflammatory cells at the implant/tissue interface, causing acute and chronic inflammation. Dense fibrotic tissue is formed due to tissue response, leading to obstructed blood sampling and hence to compromised functionality [3,4].

Hydrogel overlay, phospholipid-based biomimicry, flow-based systems, naturally derived materials, use of surfactants to reduce adhesion and co-implantation of anti-inflammatory drugs are different examples of approaches that can reduce the tissue inflammatory response [3,5]. Co-implantation of dexamethasone in poly(lactic-co-glycolic acid) (PLGA) microspheres (MS) and PLGA MS in poly(vinyl alcohol) (PVA) composites was found to suppress

* Corresponding author. Tel.: +91 22 25767746; fax: +91 22 25723480.
E-mail address: rsrivasta@iitb.ac.in (R. Srivastava).
[1] These authors contributed equally.

1742-7061/$ - see front matter © 2011 Acta Materialia Inc. Published by Elsevier Ltd. All rights reserved.
doi:10.1016/j.actbio.2011.06.053

both acute and chronic inflammatory reactions (for a period of 3 months) induced by subcutaneous implantation of a black cotton thread suture in SD rats [6]. *In vivo* release kinetics and tissue biodistribution studies were carried out by invasive intervention. It is highly beneficial if non-invasive intervention is employed for visualizing and studying the implant [7,8]. More recent advancements, like MRI, gamma camera and the use of imaging agents offer important dimensions for visualization and biodistribution of implanted particles *in vivo* [9]. MRI could be more beneficial than other modalities because of its inherent soft-tissue contrast and functional imaging capabilities especially for tumors or other lesions. The ability of the MRI to obtain non-invasive real-time images of implanted devices like biosensors, drug delivery vehicles and the device–tissue biointerface has also been demonstrated [10]. Magnetic nanoparticles (MNP) of superparamagnetic materials such as maghemite (Fe_2O_3) or magnetite (Fe_3O_4) act as excellent biocompatible MRI contrast agents and have several other applications ranging from cell separation, drug delivery and hyperthermia [11,12]. Fe_3O_4 MNP are commonly synthesized by: (i) base-catalyzed co-precipitation; (ii) thermal decomposition; and (iii) sonochemical decomposition followed by thermal treatment [13–17]. Chemically stable MNP can be obtained by coating or encapsulation in biocompatible matrix like alginate. Alginates are popular for their unique properties of organic-solvent-free processing and mild gelation [18]. Magnetic alginate microspheres (Mag-Alg-MS) have been applied for the separation and purification of α-amylase and β-amylase [19], scaffolds for drug delivery [20] and controlled drug delivery applications [18]. Iron nanoparticles containing alginate microcapsules have been synthesized and evaluated for visibility with MRI, which can help in tracking implanted microcapsules *in vivo* without invasive surgery [8]. Liu et al. [9] have described the synthesis of multifunctional alginate microspheres (Alg-MS) with magnetic and fluorescent functionalities, which have the capability of encapsulation of multifunctional moieties.

This research work aims at developing novel multifunctional co-immobilized system comprising biosensing assay, an anti-inflammatory agent and an MRI contrast agent encapsulated or entrapped in an alginate matrix using a commercially available droplet generator. Multifunctional system was prepared using glucose oxidase (GOx) immobilized in Alg-MS along with Tris (4,7-diphenyl-1,10-phenanthroline ruthenium (II) dichloride) (Rudpp) as the oxygen-sensitive dye for glucose sensing, diclofenac sodium (Diclo) as the anti-inflammatory agent and citrate-coated iron oxide (Fe_3O_4) MNP magnetic nanoparticles as the MRI agent. The gluocose biosensing mechanism is based on the detection of depletion of oxygen on the reaction of glucose with GOx using Rudpp. Diclo was used as a model non-steroidal anti-inflammatory agent to prevent implant-induced inflammation. Fe_3O_4 MNP act as the MRI contrast agent. The formulation was characterized using imaging (optical microscopy, scanning electron microscopy (SEM) and transmission electron microscopy (TEM)), X-ray diffraction (XRD), Fourier transform infrared spectroscopy (FTIR), glucose biosensing, *in vitro* drug release studies, magnetic properties (vibrating sample magnetometry (VSM) and MRI) and biocompatability studies to establish the safety and efficacy for the hypothesized objective of a single system for multiple applications.

2. Experimental section

2.1. Materials

Alginate (low viscosity, 2%), Diclo (mol. wt. 318.13), ferric and ferrous chloride, ammonia, N_2 gas, iron (II) sulphate hexahydrate, 1,10-phenanthroline monohydrate, sulphuric acid, hydroxylamine hydrochloride, ammonium acetate, glacial acetic acid, concentrated hydrochloric acid, phosphate-buffered saline tablets (PBS tablets, pH 7.4), sulphorhodamine B (SRB), D-glucose, GOx, 50 kU *Aspergillus niger*, and Rudpp were purchased from Sigma–Aldrich (India). Sodium azide was purchased from Loba Chemie Pvt. Ltd. (Mumbai, India). Dulbecco's medium Eagle's medium, fetal bovine serum, antibiotic antimycotic solutions and dialysis membrane (10–14 kDa) were purchased from Himedia Laboratories Pvt. Ltd. (India). Calcium chloride was purchased from Merck (India). All chemicals were reagent grade and used as received.

2.2. Preparation of Alg-MS containing GOx biosensor, Diclo and MRI contrast agent

MNP were prepared by mixing $FeCl_3$ and $FeCl_2$ in a molar ratio of 1.9:1 in ammonia solution (30% w/v) heated at 70 °C with constant mechanical stirring at 1000 rpm in an N_2 environment for 30 min. The mixture was heated to 90 °C after addition of citric acid and stirred for 90 min. The colored solution was cooled to room temperature and allowed to settle with the help of a magnet. The MNP formed were sonicated for 30 min after washing with acetone several times and finally resuspended in water. Alg-MS loaded with GOx–Rudpp (components of the glucose sensor), Diclo (anti-inflammatory agent) and MNP (MRI contrast agent) were prepared using an encapsulation unit in a commercially available air-driven droplet generator (Nisco encapsulation unit Var J30, Zurich, Switzerland) as per the method described by Joshi et al. [21]. Briefly, 2 mg ml^{-1} of GOx, Diclo (1 mg ml^{-1}) and MNP (1 mg) were mixed with sodium alginate solution (2% w/v). The GOx–Diclo–MNP–alginate suspension was then sprayed into a $CaCl_2$ (4% w/v) solution to gel under constant stirring using optimized instrumental parameters (nozzle diameter = 0.35 mm, flow rate of the solution/suspension = 20 ml h^{-1}, variable pressure and distance from nozzle to cross-linking solution = 10 cm). After microsphere fabrication, the particles were washed using centrifugation and placed in a solution of $\sim 3.5 \times 10^{-5}$ M Rudpp in 10 vol.% methanol in deionized water at pH 12 for 3 h. This leads to electrostatically mediated precipitation of the cationic (at basic pH), poorly water-soluble dye in the hydrated anionic alginate matrix. The Rudpp is stabilized upon resuspension of the particles in neutral-pH aqueous solutions [22].

2.3. Particle characterization

Infra-red dried MNP were characterized for size and morphology using TEM (Philips CM200, USA) by placing them on a carbon-coated copper grid at 200 kV. The mean particle size and size distributions of MNP (~100 μl) were suspended in double-distilled water and measured by dynamic light scattering (DLS; Brookhavens Instruments, USA). A blue laser (488 nm) was used as the incident radiation and scattered light was collected at 90° after suitable dark and light corrections. The mean particle diameter was determined using the intensity-weighted mode in the CONTIN algorithm in the Brookhaven software for the DLS analysis. Particle size analysis is based on obtaining a correlation function with respect to the incident light. Each measurement reported is the mean of three samples per batch of microspheres for at least three different batches. The technique is based on the scattering of incident laser light due to the random Brownian motion of the nanoparticles, which can be plotted as correlation function against time. The particle size and morphology of Alg-MS and Mag-Alg-MS were determined using a Leica DMIL optical microscope. SEM images of particles were obtained after gold sputtering in a scanning electron microscope (Hitachi S-3400, Japan) at 150–3000× with a voltage of 3 kV. Confocal laser scanning microscopy (CLSM; Olympus, Tokyo Japan) was used to characterize the Rudpp-loaded Mag-Alg-MS

and to study the distribution of dye inside the microspheres using a line scan. The XRD study was done using a Philips X'Pert Diffractometer (PW 3040/60) equipped with a 2θ compensating slit in a continuous scan mode with a step size of 0.0170° and step time of 15.18 s over an angular range 2θ of 25–80°. FTIR analysis of the dried samples of alginate MS, citric-acid-coated MNP and Mag-Alg-MS was done using the KBr pellet method in a Magna 550 spectrometer (Nicolet Instruments Corporation, USA).

2.4. Loading efficiency of GOx, Diclo and MNP in Alg-MS and enzyme activity studies

The loading efficiency of GOx/Diclo/MNP in Alg-MS was determined by calculating the amount of GOx/Diclo/MNP in supernatant after centrifugation (4000*g* for 5 min) in comparison to theoretical loading concentration. GOx loading was determined by the standard Bradford test using a Micro-2 ml protocol [23]. The Diclo loading was determined from the calibration curve of standard concentrations of Diclo in the range of 0–3 μg ml^{-1} using ultraviolet spectrophotometry (Hitachi, Japan) at 276 nm. MNP loading was determined using a phenanthroline assay of the supernatant [24]. The loading of GOx/Diclo/MNP in Alg-MS was calculated using the following formula:

$$\% \text{ Loading} = \frac{(C_t - C_s) * 100}{C_t}$$

where C_t is the theoretical loading of GOx, Diclo and Fe_3O_4, and C_s is the amount of individual components in the supernatant. GOx enzyme activity was determined using a colorimetric enzyme assay. Briefly, 2.4 ml of 0.01 M PBS, pH 7.4, containing 0.21 mM *o*-dianisidine, was combined with 500 μl β-d-glucose (100 mg ml^{-1} in 0.01 M PBS) and 100 μl peroxidase (60 Purpurogallin units ml^{-1} in deionized water). Then 100 μl of a suspension of sensors containing GOx (approximately 10^5 spheres) was added and the increase in absorbance at 500 nm was observed.

2.5. Glucose biosensing studies

The glucose sensing assay was performed using 100 μl of glucose concentrations in the range of 0–50 mM. Glucose was added to particles, the volume was made up to 1 ml and fluorescence emission scans was captured at 625 nm (λ_{ex} = 450) every 30 s for 10 min with a fluorescence spectrophotometer (Hitachi 2500, Japan). The fluorescence intensity ratio (sample (I):sample without analyte (I_0)) was plotted against the glucose concentration and the linearity established. The response time for the glucose estimation was measured using multiple measurements for a single sample (6 mM) to achieve a steady state.

2.6. In vitro drug release study

In vitro drug release studies were performed on Diclo-loaded plain Alg-MS and Mag-Alg-MS using a dialysis membrane with a molecular weight cut-off of 10–14 kDa. A dialysis membrane containing particles was transferred to a beaker containing 150 ml of PBS, pH 7.4, and 0.01% w/v sodium azide, which was maintained at 37 °C for the sink conditions of release. At different time intervals, the release medium was collected and replaced with fresh buffer. The cumulative percent release was obtained using the calibration curve prepared as described in Section 2.4.

2.7. Magnetic property evaluation studies (VSM and MRI)

The magnetic properties of MNP and Mag-Alg-MS were evaluated using VSM. The magnetization saturation was determined by plotting magnetic moment vs. field strength after exposing dried samples to a magnetic field (-2 T to 2 T). MRI studies were conducted using a Siemens MRI machine operating at 1.5 T (62.78 MHz for ^{1}H). T_1 (spin–lattice relaxation time) and T_2 (spin–spin relaxation time) determined using a fast spin echo T_2 sequence. Different concentrations (0.01, 0.03, 0.05 and 0.07 mg ml^{-1}) of MNP and Mag-Alg-MS$_{(10\ \mu m \text{ and } 60\ \mu m)}$ were imaged and evaluated for their iron content.

2.8. In vitro cytotoxicity studies

A colorimetric antiproliferative SRB assay, which estimates the cell number indirectly by staining the total cellular protein with SRB dye, was performed to assess growth inhibition. An *in vitro* cytocompatibility study of different samples (GOx–Rudpp-loaded Mag-Alg-MS, plain Alg-MS$_{(10\ \mu m \text{ and } 60\ \mu m)}$, Diclo-loaded Alg-MS$_{(10\ \mu m \text{ and } 60\ \mu m)}$, Diclo-loaded Mag-Alg-MS$_{(10\ \mu m \text{ and } 60\ \mu m)}$ MNP and Mag-Alg-MS$_{(10\ \mu m \text{ and } 60\ \mu m)}$) was carried out using L929 cells (mouse fibroblast) cell lines. The SRB assay was conducted as per the process developed by Skehan et al. and Vichai et al. [25,26]. Briefly, cells were grown, incubated, their confluency determined, and then plated, at 1×10^4 cells per well, with samples in a 96-well plate and incubated. After incubation for 48 h, the old medium was discarded, the cells were fixed using trichloroacetic acid, and the plates washed, dried and then treated with SRB in acetic acid (1%). Excess and unbound dye was removed by washing and the optical density (OD) measured using a plate reader (Thermo Electron Corporation, USA) at 560 nm. The cell viability was measured as the ratio of the OD of the sample to that of the control, and expressed as a percentage. The OD was recorded with an enzyme-linked immunosorbent assay reader at 515 nm.

3. Results and discussion

3.1. Preparation of Alg-MS containing GOx biosensor, Diclo and MRI contrast agent

Implantable biosensors have the disadvantage of fibrous capsule formation over the sensor due to tissue response. Continuous monitoring of analytes in an implantable system needs to be supported with imaging and anti-inflammatory modules for effective functioning. GOx-based sensors are the most common form of biosensors prepared for long-term glucose determination and monitoring. Researchers report several matrices for stabilized enzyme encapsulation for biosensor development; however, alginates form the most important carriers. Alg-MS support enzyme encapsulation because of mild gelation conditions. Developments of GOx-based sensors also involves the use of an oxygen-sensing element (Rudpp), which is capable of detecting changes in oxygen concentration in the microenvironment of Alg-MS during the glucose catalysis reaction. GOx and Diclo dissolve in the alginate matrix, whereas Rudpp remains electrostatically precipitated in the microspheres due to its ionic nature. Diclo is a non-steroidal anti-inflammatory agent, and is a cyclo-oxygenase and lipo-oxygenase inhibitor. Co-encapsulation of Diclo does not affect the enzyme activity of GOx, making them suitable to be used together (results not shown). In order to prepare the imaging module (MRI contrast agent), MNP were first prepared using the co-precipitation technique from aqueous Fe^{2+}/Fe^{3+} salt solutions by the addition of a base under an inert atmosphere at elevated temperature. The size, shape and composition of the MNP depend on the types of salt used (e.g. chlorides, sulfates, nitrates), the Fe^{2+}/Fe^{3+} ionic ratio, the reaction temperature, the pH value and the ionic strength of the medium. The magnetic saturation values of the magnetite nanoparticles prepared with this technique lies in the range of 30–50 emu g^{-1}. The reaction can be described as follows:

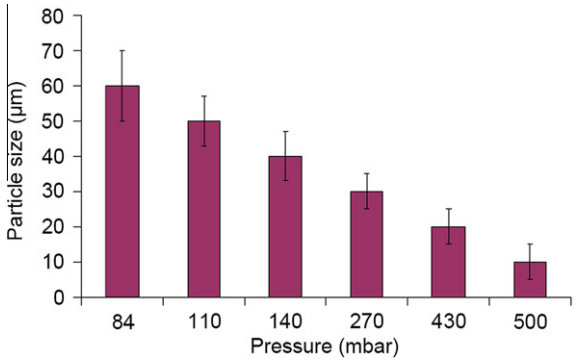

Fig. 1. Effect of increasing pressure on the formation of MNP-Alg-MS using a droplet generator, with alginate concentration (2% w/v), flow rate (10 ml h^{-1}), concentration of MNP's (0.5 mg ml^{-1}), $CaCl_2$ (4% w/v), Diclo (1 mg ml^{-1}) and GOx (2 mg ml^{-1}) (Y error bars represent the standard deviation for triplicate measurements).

$$2FeCl_3 + FeCl_2 + 8NH_4OH \rightarrow + Fe_3O_4 + 8NH_4Cl + 4H_2O$$

Magnetite nanoparticles are prone to oxidation to maghemite due to instability, hence they need to be stabilized by a coating or encapsulation. Citric acid coating and encapsulation to form Mag-Alg-MS serve to form stabilized MNP. The purpose of implantation and additional stability can be achieved by preparing Mag-Alg-MS using a protocol developed by Joshi et al. [21] and Jayant et al. [27]. Mag-Alg-MS were prepared using 2–2.5% (w/v) alginate, which can be loaded with MNP up to 5 mg ml^{-1}. The different MNP concentrations did not show any significant effect on size and stability of the MS. Fig. 1 summarizes the optimization studies for preparing Mag-Alg-MS, which indicate that increasing the atomizing pressure leads to the generation of particles of smaller size; on the other hand, the flow rate can be modulated in order to maintain the sphericity of the particles [27]. The basis of formation of smaller particles using a 0.35 mm nozzle lies in the shear, friction and formation of nuclei for droplet formation generated during atomization.

3.2. Particle characterization

TEM images confirmed that MNP were formed with sizes of 5–15 nm, in contrast to the DLS analysis, which showed a size of 30 ± 15 nm. The optical microscopy and SEM images confirmed that the MS formed are indeed spherical in shape and are of two distinct sizes: 10 ± 5 μm and 60 ± 10 μm (Fig. 2). MNP encapsulated in Alg-MS were found to be uniformly dispersed in both the 10 and 60 μm-sized Alg-MS. CLSM imaging of the biosensor suggests that Rudpp was electrostatically precipitated in the Alg-MS matrix; this distribution was confirmed using the CLSM line scan (Fig. 2). XRD patterns obtained for Fe_3O_4 nanoparticles were found to be equivalent to that of reference XRD patterns of the Fe_3O_4. The XRD intensity at 2θ values for MNP of 35.6° in Mag-Alg-MS confirms the presence of MNP. The intensity of characteristic peaks increased when the concentration of the loaded MNP was increased. FTIR spectra show the presence of C=O and OH stretching vibrations of the MS carboxyl band observed at 1697.99 cm^{-1} (C=O), 1452.77 cm^{-1} (C–O), 904.68 cm^{-1} (OH) and 1601.32 cm^{-1} (phenyl ring) in Alg-MS, MNP and Mag-Alg-$MS_{(10\ \mu m\ and\ 60\ \mu m)}$. The Fe_3O_4 molecules have a weak absorbing peak at 564.15 cm^{-1}, which confirms the presence of MNP in the Alg-MS rather than unloaded MNP (Fig. 3). The MNP absorbing peak intensity at 564.15 cm^{-1} increases when a high concentration of MNP is loaded into the Alg-MS (data not shown).

3.3. Loading efficiency of GOx/Diclo/MNP in Alg-MS and enzyme activity determination

Factors governing encapsulation and entrapment in Alg-MS include molecular weight, hydrophilicity, particle size, porosity and

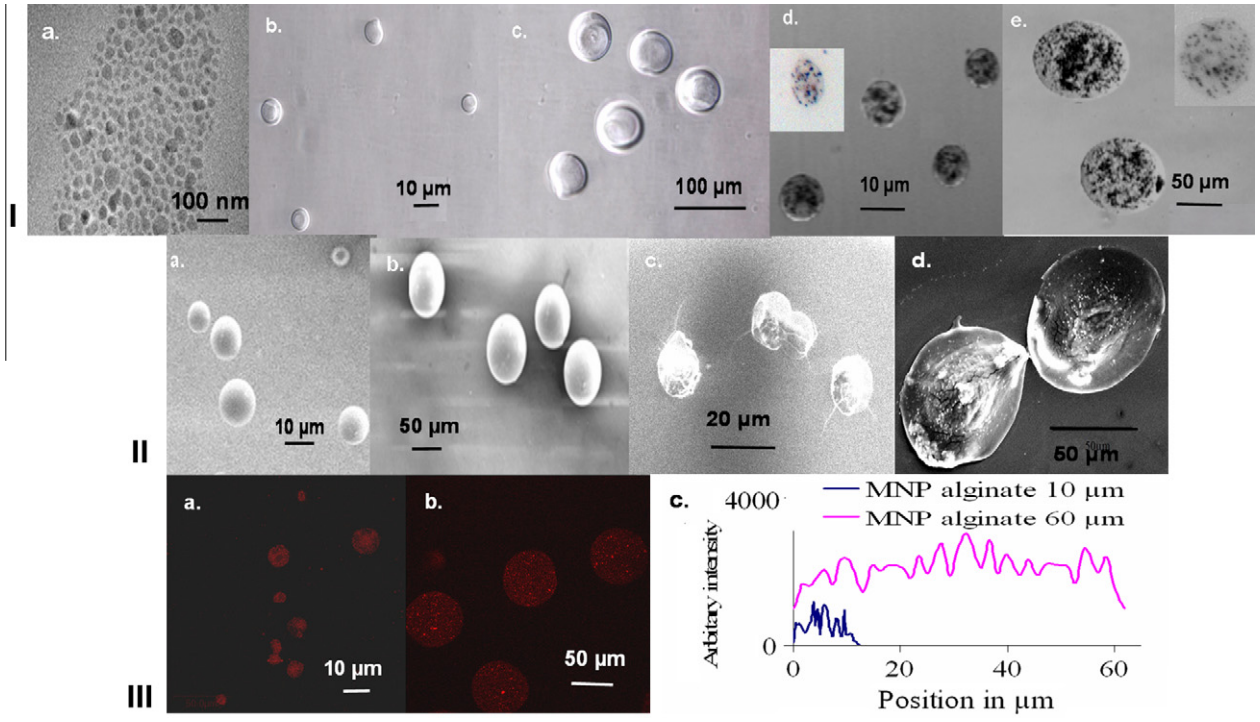

Fig. 2. (I) TEM image of (a) citric-acidcoated MNP (Fe_3O_4) and optical images of (b) plain Alg-$MS_{(10\ \mu m)}$, (c) plain Alg-$MS_{(60\ \mu m)}$, (d) Mag-Alg-$MS_{(10\ \mu m)}$ and (e) Mag-Alg-$MS_{(60\ \mu m)}$ (insets show sonicated Mag-Alg-MS); (II) SEM images of (a) plain Alg-$MS_{(10\ \mu m)}$, (b) plain Alg-$MS_{(60\ \mu m)}$, (c) Mag-Alg-$MS_{(10\ \mu m)}$ and (d) Mag-Alg-$MS_{(60\ \mu m)}$; (III) CLSM image of Rudpp loaded (a) Mag-Alg-$MS_{(10\ \mu m)}$, (b) Mag-Alg-$MS_{(60\ \mu m)}$ and (c) corresponding line scans.

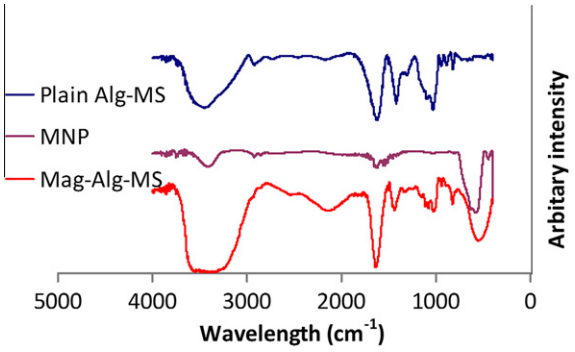

Fig. 3. FTIR spectra of MNP (----), plain Alg-MS (----) and Mag-Alg-MS (----).

concentrations of encapsulants [28,29]. GOx (mol. wt. ~150 kDa) is a high-molecular-weight water-soluble enzyme. The GOx encapsulation study showed that it gets encapsulated to an extent of 64% for a 1 mg ml^{-1} loading. Different concentrations of GOx showed no significant difference in encapsulation efficiency in the range of 0–2 mg ml^{-1}. Diclo loading was found to be higher in (plain alginate)$_{10\ \mu m}$ at all measured concentrations in comparison to other formulations. The Diclo encapsulation efficiency in MNP-loaded Alg-MS decreased due to the occupancy of MNP by ~5% in comparison to plain Alg-MS counterparts. However, Diclo encapsulation in the case of (Mag-Alg-MS)$_{60\ \mu m}$ decreased by ~3% in comparision to (Mag-Alg-MS)$_{10\ \mu m}$. As the concentration of Diclo was increased from 0.5 to 1.5 mg ml^{-1}, the encapsulation efficiency decreased by about 3–8% up to 1 mg ml^{-1}, and ~10 and ~15% at 1.5 mg ml^{-1} Mag-Alg-MS$_{(10\ \mu m \text{ and } 60\ \mu m)}$ formulations in comparison to plain Alg-MS, respectively. The encapsulation efficiency for the different formulation was in the order (plain Alg-MS)$_{10\ \mu m}$ > (plain Alg-MS)$_{60\ \mu m}$ > (Mag-Alg-MS)$_{60\ \mu m}$ > (Mag-Alg-MS)$_{10\ \mu m}$, as shown in Fig. 4b. At concentrations above 1 mg ml^{-1}, the encapsulation efficiency of both (Mag-Alg-MS)$_{10 \text{ and } 60\ \mu m}$ systems decreased dramatically in comparison to the plain Alg-MS counterparts. Different loading concentrations of MNP from 0 to 5 mg ml^{-1} showed that no significant differences were observed in (Mag-Alg-MS) of sizes 10 and 60 μm (~95%), confirming encapsulation of most of the MNP suspended in alginate (Fig. 4a). The process is thus shown to be a very efficient, industrially feasible method of encapsulation of any type of nanoparticle in Alg-MS.

Enzyme activity was evaluated to determine the effectiveness of the encapsulated enzyme for catalytic reaction. The effective activity (enzyme activity per unit protein loading) of GOx in Mag-Alg-MS was found to be around 2.3 × 10^5 AU μg^{-1} s^{-1} post-encapsulation. However, after 1 week the enzyme activity had decreased by approximately 47% from the initial value. No further significant reduction in effective activity of GOx was observed over the next 3 weeks. Layer-by-layer coating over the Alg-MS could be an effective way to maintain the GOx activity over a significant period of time.

3.4. Glucose sensing

Recently, implantable glucose biosensors ("Smart Tattoo") have been investigated for effective diabetes monitoring wherein intradermally implanted microspheres are aimed at glucose detection via transdermal interrogation using near-infrared light [30–32]. Such calibrated biosensors can aid in the accurate spot detection of blood glucose, replacing the gold-standard "finger-prick method". (Mag-Alg-MS)$_{10\ \mu m}$ microspheres selected for biosensing studies were based on the finding of Brown and McShane [33] that 10 μm particles cause lower scattering effects in comparison to 60 μm particles. Use of 1–10 μm particles provides a higher sensitivity of detection over 20–60 μm particles, whereas a higher microsphere size aids in improving the analytical range of detection of glucose [33]. The CLSM image of Mag-Alg-MS$_{(10\ \mu m \text{ and } 60\ \mu m)}$ shows that Rudpp is distributed throughout the microspheres along with the GOx (Fig. 2III a,b). The dye does not leach out more than 1% into the release medium; hence the fluorescence from Rudpp accurately reflects the mean O_2 changes throughout the

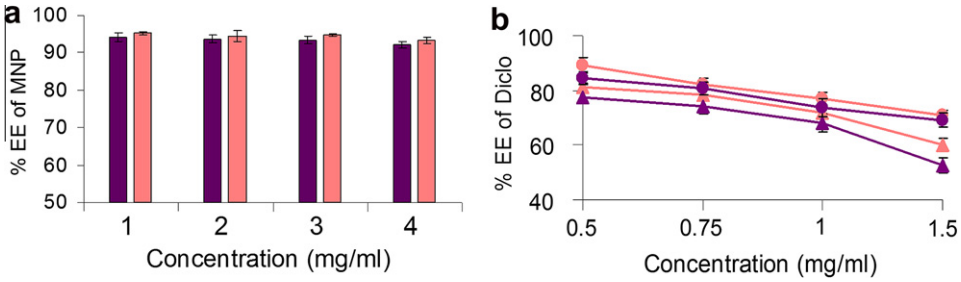

Fig. 4. (a) Encapsulation efficiency (EE) of MNP in Mag-Alg-MS$_{(10\ \mu m)}$ (■) and Mag-Alg-MS$_{(60\ \mu m)}$ (■); (b) encapsulation efficiency of Diclo in (Mag-Alg-MS)$_{10\ \mu m}$: (---▲---), (Mag-Alg-MS)$_{60\ \mu m}$ (---▲---), (Alg-MS)$_{10\ \mu m}$ (---●---) and (Alg-MS)$_{60\ \mu m}$ (---♦---). Y error bars represent the standard deviation for triplicate analysis.

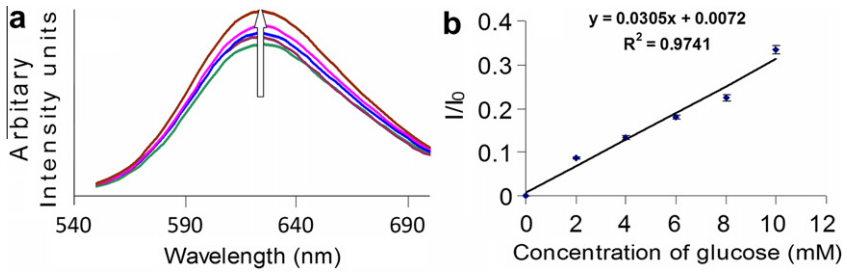

Fig. 5. Biosensing profile of glucose using GOx sensor for the concentration range. (a) Overlay of the fluorescence emission of Rudpp in response to the glucose catalytic reaction: 0 mM (-----), 2 mM (---), 4 mM(----), 6 mM(-----), 8 mM (-----) and 10 mM (----). (b) Calibration curve for the glucose sensing profile sensor particles (Y error bars represent the standard deviation for triplicate analysis).

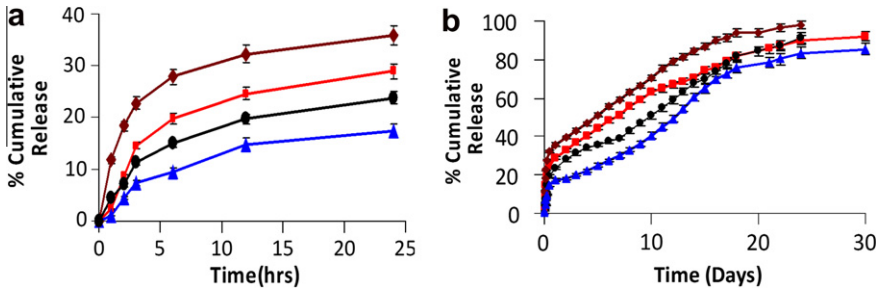

Fig. 6. (a) Diclo burst release profile from Mag-Alg-MS and plain Alg-MS: $(Mag\text{-}Alg\text{-}MS)_{10\ \mu m}$ (--♦--), $(Mag\text{-}Alg\text{-}MS)_{60\ \mu m}$ (--■--), $(Alg\text{-}MS)_{10\ \mu m}$ (--●--) and $(Alg\text{-}MS)_{60\ \mu m}$ (--▲--); and (b) Diclo controlled release profile of Mag-Alg-MS and plain Alg-MS@ $(Mag\text{-}Alg\text{-}MS)_{10\ \mu m}$ (--♦--), $(Mag\text{-}Alg\text{-}MS)_{60\ \mu m}$ (--■--), $(Alg\text{-}MS)_{10\ \mu m}$ (--●--) and $(Alg\text{-}MS)_{60\ \mu m}$ (--▲--).

sphere volume. When glucose samples were added to solutions containing Rudpp-loaded Mag-Alg-MS, the fluorescence of Rudpp at 625 nm (λ_{ex} = 450 nm) increased with increasing glucose concentration owing to oxygen consumption in the catalytic reaction between GOx and glucose (Fig. 5a). The fluorescence of the solutions was measured as a function of time until the signal reached a steady state. The biosensor performance is based on the quenching effect of ruthenium due to the presence of oxygen. The sensor showed a good regression constant of 0.974 over a range of glucose concentrations from 0 to 10 mM for the change in intensity ratio (I/I_0) with a minimum detection limit of 0.5 mM glucose (Fig. 5b).

$$\text{Glucose} + O_2 \xrightarrow{GOx} \text{Pyruvate} + H_2O_2$$

The sensitivity value for the corresponding glucose response curve was found to be 3.349% mM^{-1} at 10 mM, which was calculated from the change in intensity ratio during the reaction. The linearity was established within the range 0–10 mM. Additionally, it was revealed that increasing the enzyme concentration increases the analytical range, which can be explained by the enzyme-limited glucose catalysis at higher glucose concentrations. These results are promising, as further improvement in the sensitivity of glucose detection could be achieved by optimizing the microsphere size, the enzyme concentration and the permeability to glucose. It has been conclusively shown that glucose biosensors show a 3.3% change in peak ratio for glucose detection and can be optimized further to increase sensitivity. The "Smart Tattoo" fluorescence resonance energy transfer-based biosensor has also been investigated by Chaudhary et al. [34] for an implantable system that has shown a sensitivity of 0.52% mM^{-1} (0–30 mM range) of glucose using core-dissolved alginate microcapsules. The current method enables an ~6-fold higher sensitivity value in the range (0–10 mM) using enzyme-based sensing, which is an interesting improvement in the use of alginate microspheres. Further, the method provides the capability of detecting any analyte (based on oxygen consumption) just by changing the enzyme in the matrix.

3.5. In vitro drug release study

The co-immobilization of drugs along with other implantable systems has been previously reported by Zolnik and Burgess [35] and Srivastava et al. [36]. The former encapsulated dexamethasone in PLGA microspheres to suppress the inflammatory response, whereas the latter used dexamethasone in alginate microspheres along with an apo-gox-based glucose sensor. The tissue response was monitored over a period of 30 days and it was found that the encapsulated anti-inflammatory agent suppressed the initial tissue response. In vitro Diclo release studies from Mag-Alg-MS indicate that the burst release (BR) increases from Mag-Alg-MS.

Table 1
Summary of drug release profiles for different formulations.

Formulation and (size)	Release duration	Type of release[a]	Percentage release of Diclo
Mag-Alg-MS (60 μm)	24 h	BR	28.8
	21 days	CR	85
Mag-Alg-MS (10 μm)	24 h	BR	35.8
	14 days	CR	85
Alg-MS (60 μm)	24 h	BR	17.3
	30 days	CR	85
Alg-MS (10 μm)	24 h	BR	23.6
	20 days	CR	85

[a] BR, burst release; CR, controlled release.

The BR from $(Mag\text{-}Alg\text{-}MS)_{60\ \mu m}$ was found to be 28.89%, in comparison with 17.35% in unloaded $(Alg\text{-}MS)_{60\ \mu m}$, whereas $(Mag\text{-}Alg\text{-}MS)_{10\ \mu m}$ showed a BR value of 35.87% in comparison with 23.68% in unloaded $(Alg\text{-}MS)_{10\ \mu m}$ for a period of 24 h. The comparison also shows that a higher BR is expected for 10 μm particles than for 60 μm ones, due to the higher (about 6-fold) surface area to volume ratio, which gives a better diffusion potential for the encapsulated drugs (Fig. 6a). Nanoparticles, when encapsulated in the Alg-MS, can increase or decrease the BR. In the case of Mag-Alg-MS, the BR is increased. The higher BR in Mag-Alg-MS can be considered beneficial in countering the tissue response of the host, which is highest in the initial phases of implantation. A higher BR can prevent the attack of macrophages, polymorphonuclear leucocytes preventing the formation of a fibrotic capsule. This will prolong the life of the implant both physically and functionally. When the duration of release (CR) of 85% of Diclo is compared in all the formulations, it is found that the Mag-Alg-MS had a CR of 21 days, in comparison to 30 days for the unloaded 60 μm size (Fig. 6b). On the other hand, the 10 μm particles show CRs of 14 and 20 days for Mag-Alg-MS and Alg-MS, respectively (Table 1). The reason for the faster release from Mag-Alg-MS is due to the formation of pores and channels guided by MNP, which enables greater access to the dissolution medium in the Alg-MS. The main reason for the prolonged CR of Diclo for the 60 μm particles is the effect of the surface to volume ratio and the greater amount of drug loaded in MS in comparison to the 10 μm particles. The BR effect can be controlled using a polyelectrolyte coating applied with the layer-by-layer self-assembly technique.

3.6. Evaluation of magnetic properties

Magnetization curves give information about the magnetization saturation, hysteresis loss and susceptibility of particles. The magnetization curves (M–H loop) for MNP and Mag-Alg-MS at 25 °C

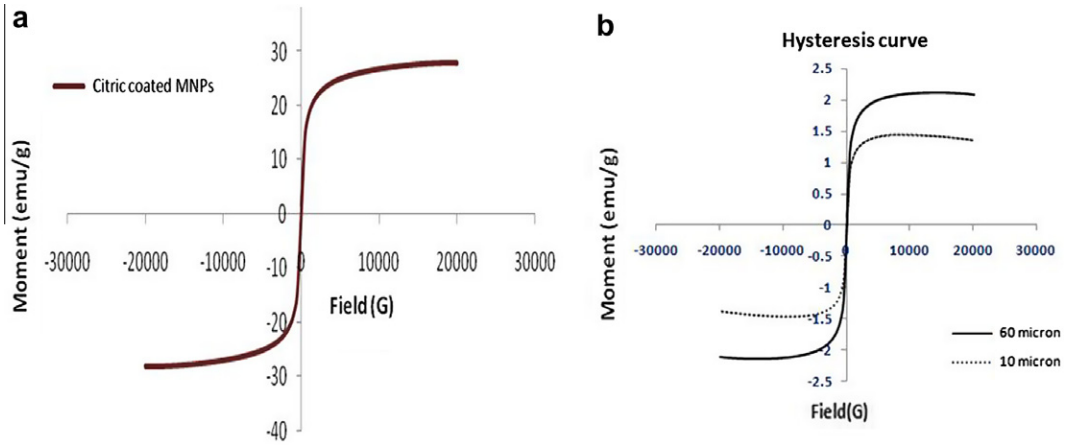

Fig. 7. VSM scans for (a) MNP and (b) Mag-Alg-MS$_{(10 \text{ and } 60\ \mu m)}$.

are described in the VSM scans, which showed that the magnetization did not reach saturation even with the maximum applied magnetic field of 10,000 Oe and that no hysteresis was found. This indicates that both nanoparticles and Mag-Alg-MS are superparamagnetic in nature and therefore can be considered in a single magnetic domain (Fig. 7). It was found that MNP-loaded Alg-MS showed magnetic moments of 1.368 and 2.09 emu g^{-1} for Mag-Alg-MS$_{10\ \mu m}$ and Mag-Alg-MS$_{60\ \mu m}$, respectively, under a magnetic field of 10,000 Oe. The magnetic moment values show a significant decrease for Mag-Alg-MS, which correlates with the observations of Denizot et al. [37] for alginate-coated MNP. The magnetic moment values can be altered according to requirements, dependent on the concentration of loading of MNP.

The MRI signal is dependent on the longitudinal (T_1) and transverse (T_2) proton relaxation times of mainly water, and therefore differences in proton relaxation times result in differences in contrast in the MRI images [38]. The intrinsic relaxation times of tissue water are dependent on the physiological environment and may be altered in pathological tissues [39]. This change may show little specificity, and could occur at a late stage of the disease. Liu et al. [9] have synthesized dual functionality composite alginate microspheres having fluorescent and MRI functions, which showed a significant contrast even at a low concentration of 0.1 mg ml^{-1}. However, these particles were prepared using an emulsification procedure that uses a batch process, with concurrent use of an organic phase and surfactants. The current method has the advantages of not using any other chemicals and providing multiple functionality.

MNP and Mag-Alg-MS were evaluated qualitatively for their magnetic contrast capability under MRI scanning. In order to keep the MNP suspended, a viscous medium was used. Of the different viscosity-maintaining agents (e.g. glycerin, agar, alginate, PVA), alginate was selected for MRI analysis. Different concentrations of MNP were suspended in 2% w/v alginate solution and imaged to determine the effect of concentration of MNP. Negative ferrofluid contains Fe_3O_4 particles because it shows all the characteristic peaks of standard Fe_3O_4 particles (Fig. 8). MRI images show that significant contrast is developed for MNP (Mag-Alg-MS)$_{(10\ \mu m \text{ and } 60\ \mu m)}$ in comparison to the control solvents. Encapsulation of MNP in Alg-MS does not affect the imaging contrast in comparison to plain Alg-MS. With increasing MNP concentration there is a corresponding increase in contrast for all three kinds of formulations (Fig. 8(II–IV)(a–d). The MRI contrast for the same concentration of MNP is slightly reduced for Mag-Alg-MS in comparison to the plain MNP, due to the encapsulated nature and the low concentrations. However, this effect is more prominent if large differences in MNP loading are evaluated. These results show that, although MNP are encapsulated in Alg-MS, they can still be used for imaging applications.

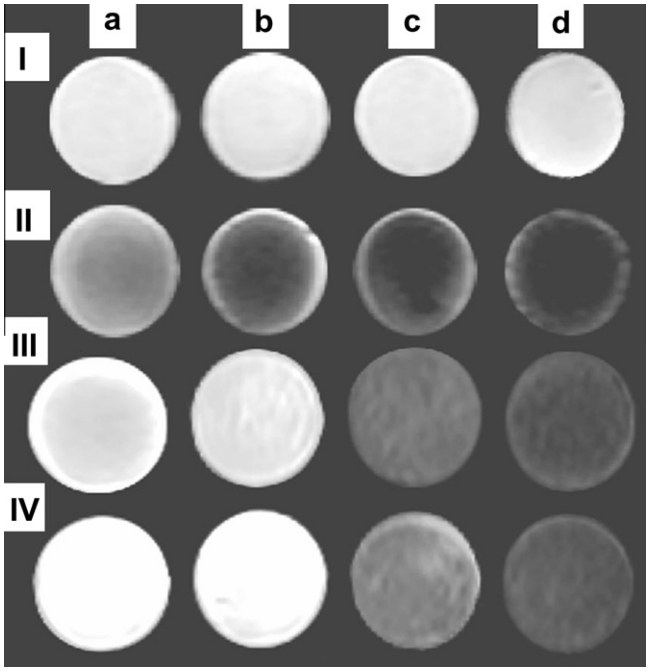

Fig. 8. MRI scans of (I) (a) water, (b) alginate solution (2% w/v), (c) (plain Alg-MS)$_{10\ \mu m}$ and (d) (plain Alg-MS)$_{60\ \mu m}$; (II) MNP with the concentrations (a) 0.01 mg ml^{-1}, (b) 0.03 mg ml^{-1}, (c) 0.05 mg ml^{-1} and (d) 0.07 mg ml^{-1}; (III) (Mag-Alg-MS)$_{60\ \mu m}$ with MNP concentrations of (a) 0.01 mg ml^{-1}, (b) 0.03 mg ml^{-1}, (c) 0.05 mg ml^{-1} and (d) 0.07 mg ml^{-1}; and (IV) (Mag-Alg-MS)$_{10\ \mu m}$ having MNP concentrations of (a) 0.01 mg ml^{-1}, (b) 0.03 mg ml^{-1}, (c) 0.05 mg ml^{-1} and (d) 0.07 mg ml^{-1}.

3.7. In vitro cytotoxicity studies

The aim of this study was to evaluate the *in vitro* cytocompatibility using the L929 mouse fibroblast cell line as this test is required by regulatory bodies for implantable devices. Different cellular aspects, like adhesion, proliferation and morphology, were analyzed in order to determine the cell viability during the culture of L929 fibroblasts with the different formulations. SRB assay indicated that no statistically significant differences were observed in the cell viability patterns of the different tested formulations. The different samples evaluated were (GOx sensor-loaded

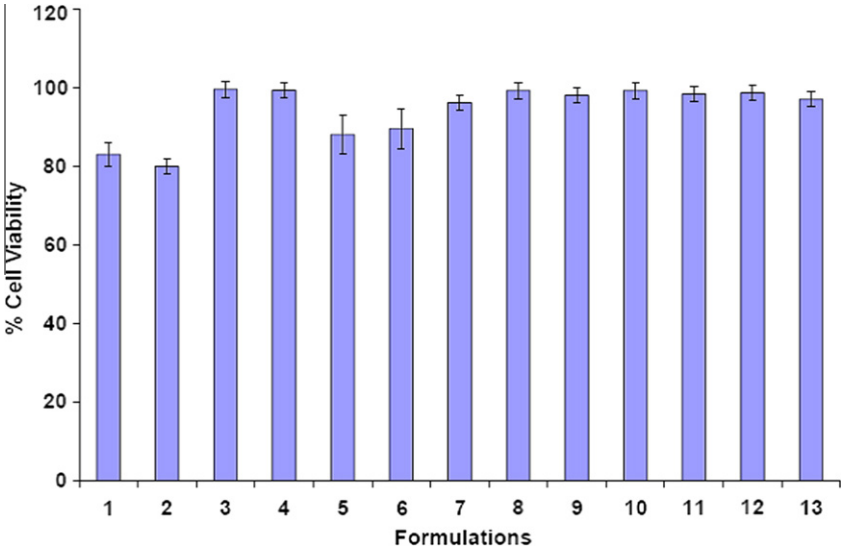

Fig. 9. Percent cell viability studies of different formulations using the L929 mouse fibroblast cell line with an SRB assay carried out after 48 h of incubation with the formulations: (1) GOX sensor-loaded Alg-MS, (2) GOX sensor-loaded Alg-MS, (3) plain Alg-$MS_{10\ \mu m}$, (4) plain Alg-$MS_{60\ \mu m}$, (5) Diclo-loaded Alg-$MS_{10\ \mu m}$, (6) Diclo-loaded Alg-$MS_{60\ \mu m}$, (7) MNP (0.5 mg ml^{-1}), (8) Mag-Alg-$MS_{10\ \mu m}$ (0.5 mg ml^{-1} MNP loading), (9) Mag-Alg-$MS_{60\ \mu m}$ (0.5 mg ml^{-1} MNP loading), (10) Mag-Alg-$MS_{10\ \mu m}$ (1 mg ml^{-1} MNP loading), (11) Mag-Alg-$MS_{60\ \mu m}$ (1 mg ml^{-1} MNP loading), (12) Mag-Alg-$MS_{10\ \mu m}$ (1.5 mg ml^{-1} MNP loading) and (13) Mag-Alg-$MS_{60\ \mu m}$ (1.5 mg ml^{-1} MNP loading) (Y error bars represent the standard deviation for $n = 4$ measurements).

Alg-$MS)_{10\ and\ 60\ \mu m}$, plain Alg-$MS_{(10\ and\ 60\ \mu m)}$, (Diclo-loaded Alg-$MS)_{10\ and\ 60\ \mu m}$, MNP (0.5 mg ml^{-1}) and Mag-Alg-$MS_{(10\ and\ 60\ \mu m)}$ (0.5–1.5 mg ml^{-1} MNP concentration). (GOx sensor-loaded Alg-$MS)_{10\ and\ 60\ \mu m}$ and (Diclo-loaded Alg-$MS)_{10\ and\ 60\ \mu m}$ showed cell viabilities of > 80 and ~94–96%, respectively. Plain Alg-$MS_{(10\ and\ 60\ \mu m)}$, (Diclo-loaded Alg-$MS)_{10\ and\ 60\ \mu m}$, MNP (0.5 mg ml^{-1}) and Mag-Alg-$MS_{(10\ and\ 60\ \mu m)}$ (0.5–1.5 mg ml^{-1} MNP concentration) all showed cell viabilities of > 95% (Fig. 9). Increasing the MNP loading in Alg-MS did not cause any changes in the cytocompatibility profile. There was no significant difference found in the biocompatibility of the MS due to the change in size of the MS from 10 to 60 μm when optimized for number of particles in each well of a 96-well plate. However, it was observed that the size of the MS may affect the cellular growth kinetics in the sense that the nutrition may get blocked due to the limited space in the 96-well plate. Therefore, this effect was reduced by optimizing the concentration of the particles added to the plates. Thus, it can be assumed that the formulations are non-detrimental for cells and can be considered for *in vivo* use.

4. Conclusions

A multifunctional system can be successfully developed using a facile technique of air-driven atomization which consists of a glucose biosensor, an anti-inflammatory agent and an MRI contrast agent encapsulated in alginate microspheres. GOx–Rudpp, Diclo and MNP were encapsulated in alginate microspheres of different sizes and characterized using imaging techniques. The system can be tuned to different sizes (10–60 μm) based on the application. TEM, optical microscopy, SEM, CLSM, XRD and FTIR confirm the presence of components inside the matrix. The loading efficiencies of GOx, Diclo and MNP were found to be ~62% (for 1 mg ml^{-1} loading), ~71% and > 90% (for 0–1.5 mg ml^{-1}), respectively. Biosensing studies for the analysis of glucose showed a well-correlated response in the range 0–10 mM for glucose, with a regression coefficient of 0. 974 and a response time of 3 min. *In vitro* drug release studies suggest that the matrix can be used for controlled release for up to 30 days to prevent inflammation. MNP loading in alginate microspheres increases the burst release and decreases the duration of release. The magnetization saturation of MNP and MNP-loaded microspheres was studied using VSM and MRI. The MNP and MNP-loaded microspheres were examined using MRI and the results show that significant contrast was observed and was readily detectable by MRI. The cytotoxicity profiles using the SRB assay also suggest favorable properties for implantable administration, with > 80% cell viability for all combinations of formulations. Such a multifunctional system has a great potential for developing implantable devices which can continuously monitor, image and respond to host tissue response.

Acknowledgement

Authors wish to acknowledge DBT Bioengineering, India for financial support.

Appendix A. Figures with essential colour discrimination

Certain figures in this article, particularly Figures 1–7, and 9, are difficult to interpret in black and white. The full colour images can be found in the on-line version, at doi:10.1016/j.actbio.2011.06.053.

References

[1] Yu B, Long N, Moussy Y, Moussy F. A long-term flexible minimally-invasive implantable glucose biosensor based on an epoxy-enhanced polyurethane membrane. Biosens Bioelectron 2006;21:2275–82.
[2] Koschinsky T, Heinemann L. Sensors for glucose monitoring: technical and clinical aspects. Diabetes Metab Res 2001;17:113–23.
[3] Hickey T, Kreutzer D, Burgess DJ, Moussy F. In vivo evaluation of a dexamethasone/PLGA microsphere system designed to suppress the inflammatory tissue response to implantable medical devices. J Biomed Mater Res 2002;61:180–7.
[4] Patil SD, Papadmitrakopoulos F, Burgess DJ. Concurrent delivery of dexamethasone and VEGF for localized inflammation control and angiogenesis. J Control Release 2007;117:68–79.
[5] Wisniewski N, Reichert M. Methods for reducing biosensor membrane biofouling. Colloids Surf B Biointerfaces 2000;18:197–219.
[6] Bhardwaj U, Sura R, Papadimitrakopoulos F. Burgess DJ. PLGA/PVA hydrogel composites for long-term inflammation control following s.c. implantation. Int J Pharm 2010;384:78–86.
[7] Ross CJ, Ralph M, Chang PL. Somatic gene therapy for a neurodegenerative disease using microencapsulated recombinant cells. Exp Neurol 2000;166:276–86.

[8] Shen F, Li AA, Gong YK, Somers S, Potter MA, Winnik FM, et al. Encapsulation of recombinant cells with a novel magnetized alginate for magnetic resonance imaging. Hum Gene Ther 2005;16:971–84.
[9] Liu J, Zhang Y, Yang T, Ge Y, Zhang S, Chen Z, et al. Synthesis, characterization, and application of composite alginate microspheres with magnetic and fluorescent functionalities. J Appl Polym Sci 2009;113:4042–51.
[10] Stenken JA, Reichert WM, Klitzman B. Magnetic resonance imaging of a tissue/implanted device biointerface using in vivo microdialysis sampling. Anal Chem 2002;74:4849–54.
[11] Boissiere M, Allouche J, Chaneac C, Brayner R, Devoisselle JM, Livage J, et al. Potentialities of silica/alginate nanoparticles as hybrid magnetic carriers. Int J Pharm 2007;344:128–34.
[12] Burke NAD, Stover HDH, Dawson FP, Lavers JD, Jain PK, Oka H. Preparation and characterization of polymer-coated magnetic nanoparticles. IEEE Trans Magn 2001;37:2600–62.
[13] Fried T, Shemer G, Markovich G. Ordered two-dimensional arrays of ferrite nanoparticles. Adv Mater 2001;13:1158–61.
[14] Hong CY, Jang IJ, Horng HE, Hsu CJ, Yao YD, Yang HC. Ordered structures in Fe_3O_4 kerosene-based ferrofluids. J Appl Phy 1997;81:4275–7.
[15] Kang YS, Risbud S, Rabolt JF, Stroeve P. Synthesis and characterization of nanometer- size Fe_3O_4 and Fe_2O_3 particles. Chem Mater 1996;8:2209.
[16] Sapieszko RS, Matijevic E. Preparation of well-defined colloidal particles by thermal decomposition of metal chelates. I. Iron oxides. J Colloid Interface Sci 1980;74:405–22.
[17] Vijayakumar R, Koltypin Y, Felner I, Gedanken A. Sonochemical synthesis and characterization of pure nanometer-sized Fe_3O_4 particles. Mat Sci Eng A-Struct 2000;286:101–5.
[18] Finotelli PV, Morales MA, Rocha-Leão MH, Baggio-Saitovitch EM, Rossi AM. Magnetic studies of iron(III) nanoparticles in alginate polymer for drug delivery applications. Mat Sci Eng C-Biomim 2004;24:625–9.
[19] Teotia S, Gupta M. Magnetite–alginate beads for purification of some starch degrading enzymes. Mol Biotechnol 2002;20:231–7.
[20] Finotelli PV, Sampaio DA, Morales MA, Rossi AM, Rocha-Leao MH. Ca alginate as scaffold for iron oxide nanoparticles synthesis. Braz J Chem Eng 2008;25:759–64.
[21] Joshi A, Keerthiprasad R, Jayant RD, Srivastava R. Nano-in-micro alginate based hybrid particles. Carbohyd Polym 2010;81:790–8.
[22] Brown JQ, Srivastava R, McShane MJ. Encapsulation of glucose oxidase and an oxygen-quenched fluorophore in polyelectrolyte-coated calcium alginate microspheres as optical glucose sensor systems. Biosens Bioelect 2005;21:212–6.
[23] Walker JM, Kruger N. The Bradford method for protein quantitation. In: Walker JM, editor. The Protein Protocols Handbook. New York: Humana Press; 2002. p. 15–21.
[24] Gutteridge JMC. Non-caeruloplasmin copper and the phenanthroline assay. Biochem J 1987;247:246–7.
[25] Skehan P, Storeng R, Scudiero D, Monks A, McMahon J, Vistica D, et al. New colorimetric cytotoxicity assay for anticancer-drug screening. J Natl Cancer Inst 1990;82:1107–12.
[26] Vichai V, Kirtikara K. Sulforhodamine B colorimetric assay for cytotoxicity screening. Nat Protoc 2006;1:1112–6.
[27] Jayant RD, McShane MJ, Srivastava R. *In vitro* and *in vivo* evaluation of anti-inflammatory agents using nanoengineered alginate carriers: towards localized implant inflammation suppression. Int J Pharm 2011;403:268–75.
[28] Srivastava R, Brown JQ, Zhu H, McShane MJ. Stable encapsulation of active enzyme by application of multilayer nanofilm coatings to alginate microspheres. Macromol Biosci 2005;5:717–27.
[29] Zhu H, Srivastava R, Brown JQ, McShane MJ. Combined physical and chemical immobilization of glucose oxidase in alginate microspheres improves stability of encapsulation and activity. Bioconjug Chem 2005;16:1451–8.
[30] Geddes CD, Lakowicz JR, McShane MJ. Microcapsules as "Smart Tattoo" glucose sensors: engineering systems with enzymes and glucose-binding sensing elements. In: Geddes CD, Lakowicz JR, editors. Glucose Sensing. New York: Springer; 2006. p. 131–63.
[31] McShane MJ, Rastegar S, Pishko M, Coté GL. Monte Carlo modeling for implantable fluorescent analyte sensors. IEEE T Bio Med Eng 2000;47:624–32.
[32] McShane MJ, Russell RJ, Pishko MV, Cote GL. Glucose monitoring using implanted fluorescent microspheres. IEEE Eng Med Biol 2000;19:36–45.
[33] Brown JQ, McShane MJ. Modeling of spherical fluorescent glucose microsensor systems: design of enzymatic smart tattoos. Biosens Bioelect 2006;21:1760–9.
[34] Chaudhary A, McShane MJ, Srivastava R. Glucose response of dissolved-core alginate microspheres: towards a continuous glucose biosensor. Analyst 2010;135:2620–8.
[35] Zolnik BS, Burgess DJ. Evaluation of in vivo–in vitro release of dexamethasone from PLGA microspheres. J Control Release 2008;127:137–45.
[36] Srivastava R, Jayant RD, Chaudhary A, McShane MJ. "Smart tattoo" glucose biosensors and effect of coencapsulated anti-inflammatory agents. J Diabetes Sci Technol 2011;5:76–85.
[37] Denizot B, Tanguy G, Hindre F, Rump E, Jacques Le Jeune J, Jallet P. Phosphorylcholine coating of iron oxide nanoparticles. J Colloid Interface Sci 1999;209:66–71.
[38] Haacke EM, Brown RW, Thompson MR, Venkatesan R. Magnetic resonance imaging: physical principles and sequence design. New York: Wiley; 1999.
[39] Caravan P, Ellison JJ, McMurry TJ, Lauffer RB. Gadolinium(III) chelates as MRI contrast agents: structure, dynamics, and applications. Chem Rev 1999;99:2293–352.